

# Interaction of magnetic field-dependent Peierls and spin-Peierls ground states in $(Per)_2[Pt(mnt)_2]$

E. L. Green, J. S. Brooks, P. L. Kuhns, and A. P. Reyes

*Department of Physics and National High Magnetic Field Laboratory, Florida State University, Tallahassee, Florida 32310, USA*

L. L. Lumata

*AIRC, UT Southwestern Medical Center, 5325 Harry Hines Blvd., NE 4.2, Dallas, Texas 75390-8568, USA*

M. Almeida

*Instituto Tecnológico e Nuclear / CFMCUL, Estrada Nacional no. 10, P-2686-953 Sacavém, Portugal*

M. J. Matos and R. T. Henriques

*Instituto de Telecomunicações, Polo de Lisboa, P1049-001 Lisboa, Portugal*

J. A. Wright and S. E. Brown

*Department of Physics and Astronomy, UCLA, Los Angeles, California 90095-1547 USA*

(Received 19 August 2011; published 23 September 2011)

The interaction of parallel conducting perylene and insulating spin-1/2  $[Pt(mnt)_2]$  molecular chains in  $(Per)_2[Pt(mnt)_2]$  is investigated through the magnetic field dependence of their coupled Peierls (charge density wave - CDW) and spin-Peierls (SP) ground states. Proton NMR is used to monitor the spin-chain behavior, and signatures in the NMR spectrum and spin-relaxation rate are compared with previous electrical transport measurements that describe the metal-insulator transition in the perylene chains associated with the CDW phase boundary. We find that the SP and CDW chains remain coupled to high fields, at variance with a simple mean-field description, and that symmetry breaking in the perylene CDW transition may drive the nearly simultaneous SP transition.

DOI: [10.1103/PhysRevB.84.121101](https://doi.org/10.1103/PhysRevB.84.121101)

PACS number(s): 71.45.Lr, 75.25.Dk, 76.60.-k

In this Rapid Communication we address the coupling of two order parameters in an organic conductor with separate itinerant and localized electron chains in high magnetic fields. For molecular chains with partially filled bands, electrical conductivity and magnetism (due to unpaired spins) are possible, and due to the low dimensionality, interactions and electronic and/or lattice instabilities can lead to a variety of ground states. Quarter-filled bands often lead to charge-ordered (CO), tetramer charge-density wave (CDW), spin-density wave (SDW), metallic or superconducting, or dimer spin-Peierls (SP) states. Half-filled bands can lead to Mott insulating or dimer spin Peierls states.

In organic conductors band filling is determined by charge transfer between donor (D) and acceptor (A) chains. (i) In DA compounds,<sup>1</sup> charge transfer can leave the donor with an unpaired spin (leading to a SP transition), while the acceptor is diamagnetic. (ii) In  $D_2A$  compounds generally the acceptor chain is a half-filled insulator, and the donor chain is a quarter-filled metal that can undergo sequential CO and SP transitions.<sup>2,3</sup> (iii) In the inorganic insulator  $CuGeO_3$  the  $Cu^{2+}$  spin-1/2 chains undergo a SP transition.<sup>4</sup> All of these show conventional SP behavior, including a uniform susceptibility<sup>5</sup> followed below the SP transition ( $T_{SP}$ ) by a rapid decrease due to the formation of a spin-singlet ground state; diffuse x-ray diffraction signals that indicate precursor and progressive dimerization above and below ( $T_{SP}$ ), respectively; and a similar magnetic-field-temperature phase diagram with a uniform ( $U$ ) phase above  $T_{SP}$ , a dimerized ( $D$ ) phase below  $T_{SP}$ , and above a critical magnetic field, an incommensurate ( $I$ ) phase where a mixture of spin-singlet and triplet regions may coexist in a soliton configuration.

In  $(Per)_2[Pt(mnt)_2]$  (Fig. 1), a unique combination of SP and CDW order parameters arises. For a  $D_2A$  material, the band in the perylene chain is quarter filled and the band in the  $Pt(mnt)_2$  chain is half filled.<sup>6</sup> The perylene chain is metallic and at low temperature undergoes a Peierls (CDW) transition to an insulating state where the perylene molecules tetramerize with wave vector  $\mathbf{q}_{Per} = \pi/2b$ . The  $Pt(mnt)_2$  chain is an insulator that undergoes a spin-Peierls transition where the Pt-dithiolate molecules dimerize with wave vector  $\mathbf{q}_{Pt} = \pi/b$ ; here the spin-1/2 ( $S = 1/2$ ) Pt moments form a spin singlet. Remarkably, even though  $\mathbf{q}_{Pt} = 2\mathbf{q}_{Per}$ , diffuse x-ray scattering, specific heat, and electrical transport indicate that both the CDW and SP transitions occur at the same, or at very similar temperature<sup>7,8</sup> (hereafter  $T_{SP-CDW}$ ). This observation suggests that the two chains are strongly coupled, even with the mismatch in  $\mathbf{q}$  vectors. In light of this, one-<sup>9</sup> and two-chain<sup>10</sup> one-dimensional Kondo lattice models have been considered in treating the coupling of the itinerant electrons and localized spins associated with the onset of the  $T_{SP-CDW}$  transition, but at present there is no complete theory that treats the two-chain  $(Per)_2[Pt(mnt)_2]$  case. In the work presented here, we show that even at high magnetic fields this coupling persists, and that the initial tetramerization in the perylene chains may promote the stabilization of the SP dimerization and the resulting spin-singlet ground state.

Since mean-field theory predicts<sup>11</sup> the suppression of the SP transition with magnetic field should be about twice that of the CDW transition, the degree of interchain coupling may show up in the magnetic field dependence, as described in Fig. 1(a). In addition, the magnetic field dependence of the resistive transition in  $(Per)_2[Au(mnt)_2]$  ( $S = 0$ ) where

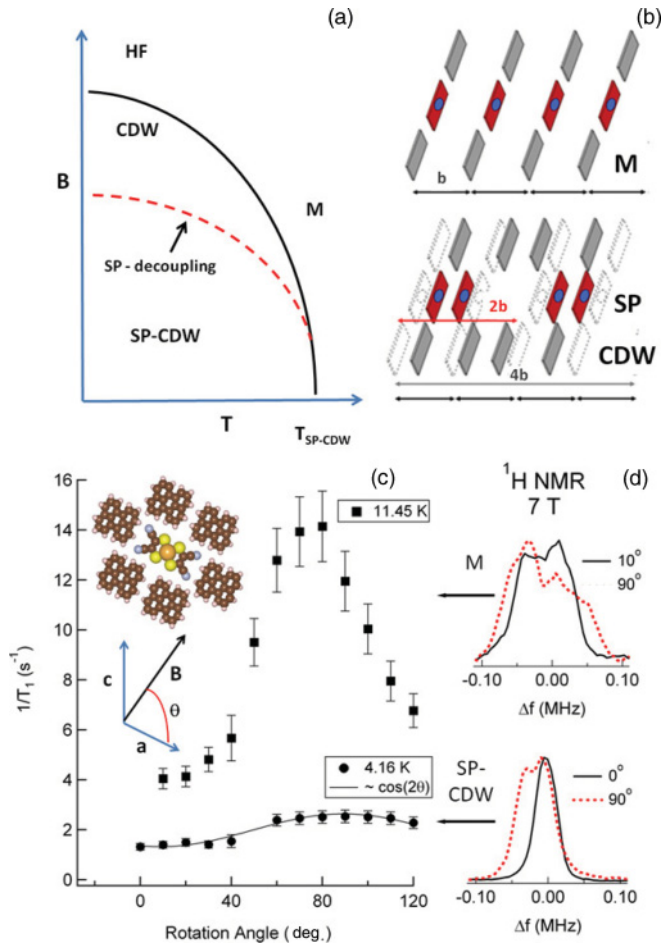


FIG. 1. (Color online) Spin-Peierls (SP) and charge-density wave (CDW) transitions in  $(Per)_2[Pt(mnt)_2]$ . (a) Hypothetical mean-field B-T phase boundaries for decoupling (with magnetic field) of the CDW (solid line) and SP (dashed line) phases, starting from the case  $T_{SP} = T_{CDW} = T_{SP-CDW}$  for  $B = 0$  T. M and HF refer to metallic and high-magnetic-field phases, respectively. (b) Configurations of the perylene (outer planes) and  $Pt(mnt)_2$  (inner plane) molecular chains along the  $b$  axis in the metallic and SP (dimerized) and CDW (tetramerized) configurations. (c)  $^1H$  relaxation time ( $1/T_1$ ) vs field orientation in the high-temperature M and low-temperature SP-CDW states for a  $(Per)_2[Pt(mnt)_2]$  single crystal at 7 T. The anisotropy in  $1/T_1$  follows a  $\cos(2\theta)$  dependence. Crystal structure:  $Pt(mnt)_2$  (Pt at center); outer ring, perylene molecules with peripheral protons. Schematic: field orientation in the crystallographic  $a$ - $c$  plane with  $B \perp b$ . (d)  $^1H$  spectra for two different field orientations in the M and SP-CDW phases.

only a CDW occurs, and  $(Per)_2[Pt(mnt)_2]$  ( $S = 1/2$ ) show dramatic differences.<sup>12,13</sup> For the  $S = 1/2$  case additional structure appears at high fields [(the “HF” phase in Fig. 1(a)], where a second high-resistance state accompanied by steplike features in the magnetoresistance and magnetization appear. This may indicate a continuing interaction of itinerant and localized electrons as the SP singlet state begins to break down. Electrical transport measurements directly probe the behavior of the perylene (conduction electron) chains. Hence the motivation for the present work is to use high-field NMR to explore the behavior of the localized Pt spin chain directly ( $^{195}Pt$ -NMR) or indirectly through the peripheral protons

on the perylene molecules ( $^1H$ -NMR) for comparison with previous transport measurements.

All studies were carried out with a standard NMR spectrometer using spin-echo methods. Both superconducting (17 T) and resistive (31 T) magnets were used with an interchangeable probe that allowed top-tuning and sample rotation in standard helium cryostats. For the  $^1H$  measurements, a single crystal ( $5 \times 0.1 \times 0.05$  mm) was used in a microcoil with an estimated filling factor of 50%. The long  $b$  axis of the crystal was collinear with the coil and perpendicular to the magnetic field. Single-crystal rotation was in the  $a$ - $c$  plane. We describe our measurements in general terms for the three regions of the  $(Per)_2[Pt(mnt)_2]$  phase diagram: the metallic phase (M) is generally above 8 K; the SP-CDW phase is below 8 K and/or below 20 – 25 T, and the high-field (HF) phase is below 8 K and above 20 – 25 T. These three regions roughly correspond to the  $U$ ,  $D$ , and  $I$  phases in traditional SP materials.

In Figs. 1(c) and 1(d) the angular dependence of the spin relaxation rate  $1/T_1$  and select spectra are shown for  $^1H$  for temperatures in the SP-CDW and M phases. The  $1/T_1 = a + b \cos(2\theta)$  dependence is characteristic of dipolar coupling. In the SP-CDW phase (7 T, 4.16 K), for  $\theta = 0^\circ$  the spectrum collapses to one line. In the M phase (7 T, 11.45 K) the spectrum has two lines, even at  $\theta = 0^\circ$ , which broaden into multiple lines for  $\theta = 90^\circ$ . The significantly greater multiple splitting and broadening in the M phase shows that the spin-singlet state has been broken. The small size and needle morphology of the sample made it difficult to determine the  $a$  and  $c$  axes precisely. Based on computed spectra and relaxation rates vs field orientation in the  $a$ - $c$  plane, we find that the second moment and  $1/T_1$  are at a minimum near  $B//a$ . This is the direction (i.e.,  $\theta = 0^\circ$ ) used for all of the  $^1H$  NMR measurements vs temperature and magnetic field reported in Figs. 2 and 3 below.

Representative temperature-dependent  $^1H$  spectra and  $1/T_1$  are shown for the transition in temperature from SP-CDW to M for  $B = 7$  T [Figs. 2(a)– 2(c)]. Figure 2(a) shows that upon crossing the main SP-CDW phase boundary the spectrum changes from a single line characteristic of a spin-singlet SP state to multiple lines indicated as 1 and 2 [Fig. 2(b)], with a splitting consistent with the size of the dipole field ( $\sim 0.9 \text{ T} \times \text{\AA}^3/r^3$ ) produced by a Pt spin at the average distance ( $r \sim 8 \text{ \AA}$ ) to the proton sites.<sup>14</sup> The spin-relaxation rate  $1/T_1$  [Fig. 2(c)] shows a change of slope at the transition.

The magnetic field dependence of the spectra and relaxation rates are shown in Figs. 2(d)– 2(f) at 3.1 K, starting from low fields in the SP-CDW phase up to 26 T in the HF phase. Changes in the spectra indicate a transition from the singlet state to multiple features (1, 2, and 3 are shown) in the vicinity of 18 T, and this coincides with a feature in the field dependence of  $1/T_1$  as well. Of note is that the third feature (3) broadens with increasing magnetic field.<sup>15</sup>

Our results are summarized in Fig. 3, where we compare the features of the NMR experiment with previous electrical transport and magnetization studies of the  $(Per)_2[Pt(mnt)_2]$  B-T phase diagram.

In our initial investigation (Ref. 16),  $^{195}Pt$  NMR was investigated on a nonaligned assembly of small single crystals of  $(Per)_2[Pt(mnt)_2]$ . The  $^{195}Pt$  NMR spectra and relaxation times were only observable well within the SP-CDW phase,

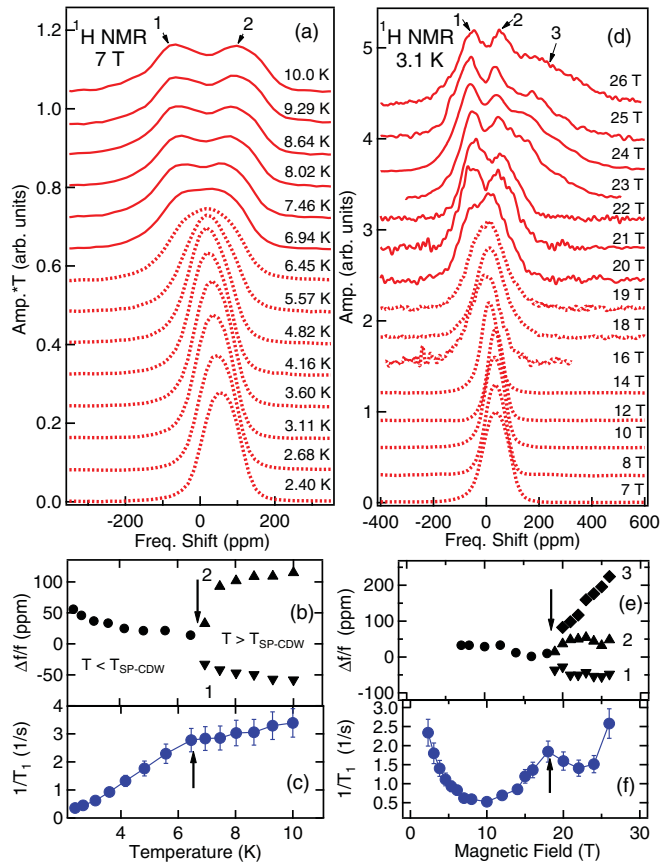


FIG. 2. (Color online) Temperature- and magnetic-field-dependent  $^1\text{H}$  NMR spectra and relaxation rates in  $(\text{Per})_2[\text{Pt}(\text{mnt})_2]$ . Left panels - 7-T data vs temperature: (a) Spectra below (dashed lines) and above (solid lines)  $T_{\text{SP-CDW}}$  at 7 T. (b) Spectral peak positions showing the splitting into multiple (1 and 2 indicated) features above 6 K. (c) Spin relaxation rate  $1/T_1$  vs  $T$  showing a break in slope above 6 K. Right panels - 3.1-K spectra vs field: (d) Changes in spectra as the field is increased from the SP-CDW phase (dashed lines) into the high-field (HF) phase (solid lines). (e) Spectral peak features 1, 2, and 3 appearing above 18 T. (f) Spin relaxation rate  $1/T_1$  vs magnetic field. Arrows: temperature and field positions of transitions.

and as the SP-CDW boundary was approached the signal amplitude vanished quickly, either with increasing temperature [ $A(14.8 \text{ T}) \sim 1/T^4$ ] or with field [ $A(1.8 \text{ K}) \sim e^{-B}$ ]. This implies that very strong de-phasing fluctuations appear at the Pt site in the spin-singlet SP chain structure near the phase boundary. Although consistent with the breaking of the SP singlet state, the vanishing  $^{195}\text{Pt}$  signal precluded any accurate determination of relaxation times near the boundary, and no signal was observable at any temperature (above 5 K) or field (above 23 T) outside the SP-CDW region. In contrast, the  $^1\text{H}$  signal, due to the distance ( $\geq 4.8 \text{ \AA}$ ) between the protons and Pt spins, survives the phase transition out of the SP-CDW phase. Comparison with previous complementary studies<sup>10</sup> of  $(\text{Per})_2[\text{Au}(\text{mnt})_2]$  ( $S = 0$ ) and  $(\text{Per})_2[\text{Pt}(\text{mnt})_2]$  ( $S = 1/2$ ) shows that the behavior of the  $^1\text{H}$  NMR data is primarily sensitive to the spin configurations and dynamics of the  $[\text{Pt}(\text{mnt})_2]$  chains. Hence the behavior of the  $^1\text{H}$  spectra and relaxation rates gives a clear indication of the SP phase boundary as the singlet ground state is broken.

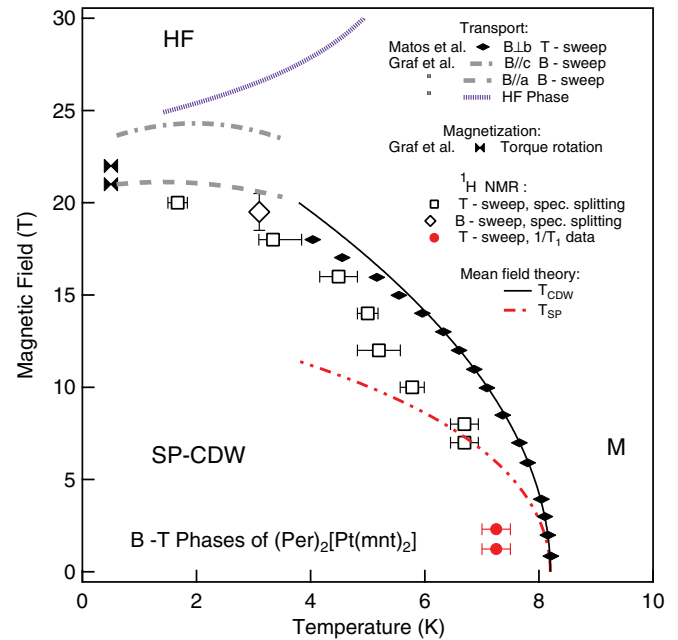


FIG. 3. (Color online) Comparison of magnetic-field-dependent phase boundaries of  $(\text{Per})_2[\text{Pt}(\text{mnt})_2]$  determined from electrical transport and torque measurements (Refs. 17 and 13),  $^1\text{H}$  NMR measurements (this work), and mean-field predictions<sup>11</sup> for  $T_{\text{CDW}}$  and  $T_{\text{SP}}$ . The  $^1\text{H}$  NMR data represent the temperature and field where the spectra split from single to double peaks with increasing temperature (open squares) or magnetic field (open diamond). Low-field  $1/T_1$  data where a distinct slope change in  $1/T_1$  vs  $T$  is observed are also shown.

This is shown for the onset of splitting of the spectra for temperature sweeps (squares) and the field sweep (diamond) in Fig. 3. For comparison, the phase boundary determined from temperature-dependent electrical transport measurements,<sup>17</sup> and magnetoresistance and torque magnetization studies<sup>13</sup> are also presented.

The main result of the present work is that even with the uncertainties<sup>18</sup> of the determination of the SP phase boundary (typically  $\pm 1 \text{ T}$  and  $\pm 1 \text{ K}$ ), the NMR signatures follow the magnetic-field-dependent CDW boundary determined from electrical transport and magnetic torque measurements. Hence the SP and CDW order parameters remain coupled at high fields. Otherwise the NMR data would show a SP transition at a much lower magnetic field ( $\sim 14 \text{ T}$  or less). Conversely, the influence of the  $[\text{Pt}(\text{mnt})_2]$  spin chains on the field dependence of the CDW boundary determined from electrical transport is small, as previously discussed by Almeida and Henriques.<sup>19</sup> This implies that the onset of tetramerization in the perylene chains creates the environment that triggers the symmetry breaking and dimerization in the  $[\text{Pt}(\text{mnt})_2]$  chains, which might otherwise remain paramagnetic to lower temperatures (typically  $T_{\text{sp}} \ll \Theta_{\text{Curie-Weiss}} \sim 20 \text{ K}$ ).<sup>10</sup>

The details of the coupling remain unresolved, but a possible scenario<sup>7</sup> is the presence of weak  $4k_F$  character in the perylene chains that can couple to the  $[\text{Pt}(\text{mnt})_2]$  chains. This is, in fact, a general characteristic of related organic conductors in this class, where  $4k_F$  instabilities can lead to CO and SP ground states,<sup>3</sup> driven by Coulombic interactions. Moreover, based on the linear scaling of  $1/T_1$  vs  $T\chi$ ,

Bourbonnais *et al.*<sup>10</sup> show that the spin degrees of freedom remain diffusive and weak until  $T_{\text{SP-CDW}}$ , and hence it is hard to see how the SP dimerization can be a result of, for instance, quantum spin dynamics alone. We note, however, that since electron paramagnetic resonance (EPR) studies indicate an interaction between the itinerant and localized spins, an exchange interaction might be involved in the cooperative SP-CDW transition. It will be important to consider how the possibility that the Peierls transition drives the spin-Peierls transition fits in with the model of Xavier *et al.*,<sup>9</sup> who predict, using a single-chain Kondo model, that a Ruderman-Kittel-Kasuya-Yosida (RKKY) interaction between the localized moments is facilitated by itinerant electrons, inducing dimerization in the SP chain.

This work lays the foundation for future studies of the effects of coupled order parameters in high magnetic fields. The data in Figs. 2(d) and 2(e) show that after the SP state

starts to break above 18 T, there is a further broadening and evolution of the spectra (feature 3) that indicates a Zeeman-like increase of local moment strength. This is characteristic of the generation of triplet excitations in the incommensurate (I) phase.<sup>3</sup> Although a non-SP model has been proposed,<sup>20</sup> it is interesting to speculate about how a changing periodic singlet-triplet soliton configuration might affect the anomalous steplike behavior<sup>13</sup> of the electrical transport above 20 T, should significant interchain coupling still be present. Further work to 45 T is planned in the near future to explore this possibility.

This work was supported in part by NSF DMR-0602859 and 1005293 (JSB), by FCT (Portugal) PTDC/FIS/113500/2009 (MA), by NSF DMR-0804625 (SEB), and performed at the National High Magnetic Field Laboratory (supported by NSF DMR-0654118, by the State of Florida, and the DOE).

- 
- <sup>1</sup>J. W. Bray, H. R. Hart, L. V. Interrante, I. S. Jacobs, J. S. Kasper, G. D. Watkins, S. H. Wee, and J. C. Bonner, *Phys. Rev. Lett.* **35**, 744 (1975).
- <sup>2</sup>D. S. Chow, F. Zamborszky, B. Alavi, D. J. Tantillo, A. Baur, C. A. Merlic, and S. E. Brown, *Phys. Rev. Lett.* **85**, 1698 (2000).
- <sup>3</sup>F. Zamborszky, W. Yu, W. Raas, S. E. Brown, B. Alavi, C. A. Merlic, and A. Baur, *Phys. Rev. B* **66**, 081103 (2002).
- <sup>4</sup>M. Hase, I. Terasaki, and K. Uchinokura, *Phys. Rev. Lett.* **70**, 3651 (1993).
- <sup>5</sup>G. Castilla, S. Chakravarty, and V. J. Emery, *Phys. Rev. Lett.* **75**, 1823 (1995).
- <sup>6</sup>L. Alcacer, H. Novais, F. Pedroso, S. Flandrois, C. Coulon, D. Chasseau, and J. Gaultier, *Solid State Commun.* **35**, 945 (1980).
- <sup>7</sup>V. Gama, R. T. Henriques, G. Bonfait, M. Almeida, S. Ravy, J. P. Pouget, and L. Alcacer, *Mol. Cryst. Liq. Cryst.* **234**, 171 (1993).
- <sup>8</sup>G. Bonfait, M. J. Matos, R. T. Henriques, and M. Almeida, *J. Phys.* **IV 3**, 251 (1993).
- <sup>9</sup>J. C. Xavier, R. G. Pereira, E. Miranda, and I. Affleck, *Phys. Rev. Lett.* **90**, 247204 (2003).
- <sup>10</sup>C. Bourbonnais, R. T. Henriques, P. Wzietek, D. Königter, J. Voiron, and D. Jerome, *Phys. Rev. B* **44**, 641 (1991).
- <sup>11</sup>J. W. Bray, L. V. Interrante, I. S. Jacobs, and J. C. Bonner, *The Spin-Peierls Transition, in Extended Linear Chain Compounds*, edited by T. S. Miller (Plenum Press, New York and London, 1983), p. 353. The general expressions for the suppression of the transition temperature with magnetic field are  $\Delta T_{\text{CDW}}/T_{\text{CDW}}(0) = -\gamma[\mu_B B/k_B T_{\text{CDW}}(0)]^2$ , and  $\Delta T_{\text{SP}}/T_{\text{SP}}(0) = -\delta[\mu_B B/k_B T_{\text{SP}}(0)]^2 - \kappa[\mu_B B/k_B T_{\text{SP}}(0)]^4$ . In this paper we have used  $\gamma = 0.2$ ,  $\delta = 0.44$ , and  $\kappa = 0.2$ .
- <sup>12</sup>D. Graf, J. S. Brooks, E. S. Choi, S. Uji, J. C. Dias, M. Almeida, and M. Matos, *Phys. Rev. B* **69**, 125113 (2004).
- <sup>13</sup>D. Graf, E. S. Choi, J. S. Brooks, R. T. Henriques, M. Almeida, and M. Matos, *Phys. Rev. Lett.* **93**, 076406 (2004).
- <sup>14</sup>The spin density extends in the the  $[\text{Pt}(\text{mnt})_2]^{-1}$  anion, being mainly in Pt (0.356), and in the four sulfur (0.458 total) atoms. (J. Novoa, private communication.) In addition, there are as many as 24 inequivalent proton sites, making a detailed assignment of the spectral features difficult.
- <sup>15</sup>The bandwidth of the NMR probe decreases with increasing frequency, and data above 22 T were acquired with a frequency sweep method to cover the broadening line, accounting for the slight difference in line shape between 22 and 23 T. For  $1/T_1$  measurements above 22 T, the entire linewidth was saturated and the recovery monitored at the center frequency.  $1/T_1$  does not change appreciably over the spectrum since the spins are dipole-coupled and strongly correlated.
- <sup>16</sup>L. L. Lumata, Ph.D. dissertation, Florida State University, 2008; [<http://etd.lib.fsu.edu/theses/available/etd-11102008-162533/>].
- <sup>17</sup>M. Matos, G. Bonfait, R. T. Henriques, and M. Almeida, *Phys. Rev. B* **54**, 15307 (1996).
- <sup>18</sup>High-frequency (NMR) and dc (electrical transport) measurements can yield differences in transition temperature determinations. See, for instance, L. L. Lumata, J. S. Brooks, P. L. Kuhns, A. P. Reyes, S. E. Brown, H. B. Cui, and R. C. Haddon, *Phys. Rev. B* **78**, 020407 (2008).
- <sup>19</sup>M. Almeida and R. T. Henriques, *Perylene Based Conductors, in Handbook of Organic Conductive Molecules and Polymers*, edited by H. Nalwa (Wiley, New York, 1997), pp. 87–149.
- <sup>20</sup>A. G. Lebed and S. Wu, *Phys. Rev. Lett.* **99**, 026402 (2007).